
Since January 2020 Elsevier has created a COVID-19 resource centre with free information in English and Mandarin on the novel coronavirus COVID-19. The COVID-19 resource centre is hosted on Elsevier Connect, the company's public news and information website.

Elsevier hereby grants permission to make all its COVID-19-related research that is available on the COVID-19 resource centre - including this research content - immediately available in PubMed Central and other publicly funded repositories, such as the WHO COVID database with rights for unrestricted research re-use and analyses in any form or by any means with acknowledgement of the original source. These permissions are granted for free by Elsevier for as long as the COVID-19 resource centre remains active.

Virology 552 (2021) 43–51

Contents lists available at ScienceDirect

Virology

journal homepage: www.elsevier.com/locate/virology

# Epithelial-mesenchymal transition of absorptive enterocytes and depletion of Peyer's patch M cells after PEDV infection

Ya-Mei Chen [a], Emma T. Helm [b], Jennifer M. Groeltz-Thrush [c], Nicholas K. Gabler [b], Eric R. Burrough [c,*]

[a] Department of Veterinary Pathology, College of Veterinary Medicine, Iowa State University, Ames, IA, USA
[b] Department of Animal Science, Iowa State University, College of Agriculture and Life Sciences, Ames, IA, USA
[c] Department of Veterinary Diagnostic and Production Animal Medicine, College of Veterinary Medicine, Iowa State University, Ames, IA, USA

ARTICLE INFO

*Keywords:*
Intestine
Epithelial-mesenchymal transition
Enteric coronavirus
Microfold cell
Weaned pig

ABSTRACT

This study focused on intestinal restitution including phenotype switching of absorptive enterocytes and the abundance of different enterocyte subtypes in weaned pigs after porcine epidemic diarrhea virus (PEDV) infection. At 10 days post-PEDV-inoculation, the ratio of villus height to crypt depth in both jejunum and ileum had restored, and the PEDV antigen was not detectable. However, enterocytes at the villus tips revealed epithelial-mesenchymal transition (EMT) in the jejunum in which E-cadherin expression decreased while expression of N-cadherin, vimentin, and Snail increased. Additionally, there was reduced expression of actin in microvilli and Zonula occludens-1 (ZO-1) in tight junctions. Moreover, the protein concentration of transforming growth factor β1 (TGFβ1), which mediates EMT and cytoskeleton alteration, was increased. We also found a decreased number of Peyer's patch M cells in the ileum. These results reveal incomplete restitution of enterocytes in the jejunum and potentially impaired immune surveillance in the ileum after PEDV infection.

## 1. Introduction

Porcine epidemic diarrhea virus (PEDV) is an enveloped, single-stranded RNA virus that belongs to family Coronaviridae, subfamily Orthocoronavirinae, genus Alphacoronavirus, and subgenus Pedacovirus. The virus infects all ages of pigs via fecal-oral transmission. Similar to other porcine enteric coronaviruses, PEDV infection causes vomiting and diarrhea, particularly in nursing piglets and weaned pigs (Debouck et al., 1981; Niederwerder and Hesse, 2018). The virus replicates in absorptive epithelial cells of the small intestine and induces apoptosis and necrosis, epithelial cell sloughing, and retraction of villus stromal cores which leads to a decreased villus height to crypt depth ratio (VH:CD) (Debouck et al., 1981; Kim and Lee, 2014). Moreover, PEDV infection reduces a number of enterocyte subtypes related to innate immunity, including goblet cells, villus microfold (M) cells, and Peyer's patch M cells (Jung and Saif, 2017; Chen et al., 2020). Such localized damage could result in disturbed intestinal homeostasis, including disruption of the microbiota (Liu et al., 2015; Koh et al., 2015). Studies have further demonstrated that PEDV-infected weaned pigs have reduced average daily gain (ADG) and average daily feed intake (ADFI) yet the mechanisms are unclear (Curry et al., 2017a, 2018). Collectively, these findings suggest that PEDV infection contributes to a profound and likely persistent alteration in small intestinal function. Therefore, evaluation of changes in different enterocyte subtypes in the small intestine after PEDV infection is warranted.

Enterocytes in the mucosa interconnect to each other by tight junctions, adherens junctions, and desmosomes, forming a complete intestinal barrier. PEDV infection results in the loss of tight junction proteins, including ZO-1, ZO-2, occludin, and some claudins, indicating impaired intestinal integrity (Jung et al., 2015a; Schweer et al., 2016; Curry et al., 2017b; Zong et al., 2019). In addition to damaging tight junctions, PEDV infection contributes to disorganization of epithelial cadherin (E-cadherin) and microfilaments (Jung et al., 2015a; Zhou et al., 2017; Zhao et al., 2014). E-cadherin is a critical component in the adherens junction, and deprivation of E-cadherin is one of features of epithelial-mesenchymal transition (EMT) in epithelial cells. EMT is a process whereby epithelial cells lose the expression of E-cadherin but concurrently express vimentin and neural cadherin (N-cadherin),

* Corresponding author. Department of Veterinary Diagnostic and Production Animal Medicine, College of Veterinary Medicine 1800 Christensen Drive, Ames, IA, USA, 50011-1134.
*E-mail address:* burrough@iastate.edu (E.R. Burrough).

https://doi.org/10.1016/j.virol.2020.08.018
Received 26 June 2020; Received in revised form 18 August 2020; Accepted 31 August 2020
Available online 11 October 2020
0042-6822/© 2020 Elsevier Inc. All rights reserved.

resulting in cell contact dissolution and actin reorganization (Eastham et al., 2007; Ullmann et al., 2007). As cells undergo EMT, microfilaments are rearranged, leading to the disappearance of cellular polarity. Persistent transmissible gastroenteritis virus (TGEV) infection induces EMT and this has been shown to promote *Escherichia coli* infection (Xia et al., 2017). *Salmonella* spp. Infection also stimulates enterocytes to undergo EMT for enhancing bacterial invasion (Tahoun et al., 2012). Since disorganized E-cadherin and microfilaments were observed in PEDV infection, EMT induced by PEDV warrants investigation and could help reveal the possibility of superinfections (secondary bacterial infections).

Therefore, herein we aimed to characterize small intestinal restitution post-PEDV infection by screening for evidence of EMT in enterocytes at villus tips and via analyzing the abundance of different enterocyte subtypes in both jejunum and ileum. We have hypothesized that there would be incomplete intestinal restitution in weaned pigs following PEDV infection as evident by increased EMT.

## 2. Materials and methods

### 2.1. Animals and experimental design

All experimental protocols were approved by the Institutional Animal Care and Use Committee at Iowa State University (IACUC# 8-17-8580-S). A total of 64 four-week-old, conventional weaned pigs were selected from a PEDV negative herd. Pigs were randomly allotted to PEDV-infected (n = 40) and sham-inoculated (control; n = 24) treatments and were housed in separated rooms by treatment with strict biosecurity and biocontainment. Animals were given free access to water and ad libitum fed a diet that met or exceeded NRC requirements for this size of pig (Council, 2012) throughout the study period. Pigs were acclimated for 4 days before inoculation.

On day 0 post-inoculation (DPI), the PEDV-infected treatment group was inoculated orally with 10 mL of $10^4$ $TCID_{50}$/ml PEDV isolate (USA/IN19338/2013) per pig, while the control treatment pigs received 10 mL of sterile media sham (Thomas et al., 2015; Chen et al., 2016a). At DPI 2, 4, 6, and 10, 10 PEDV-infected and 6 control pigs were randomly chosen and euthanized via captive bolt and exsanguination for fixed and frozen jejunum and ileum tissue collection. For frozen tissue, jejunum and ileal sections were excised, flushed with phosphate buffered saline (PBS), snap frozen in liquid nitrogen and stored in a −80 °C freezer until further use. Fixed tissue procedures are described below. The clinical disease incidence, fecal virus shedding data, jejunum and ileum VH:CD ratios, and PEDV antigen detection by immunohistochemistry (IHC) at DPI 2, 4, 6 and 10 have been reported in a previous paper (Chen et al., 2020). Pigs at DPI 10 were selected in the present study to assess intestinal restitution at the end of the study duration.

### 2.2. Tissue collection and Alcian Blue-PAS stain

Tissue samples of jejunum and ileum were formalin-fixed, paraffin-embedded, sectioned at 4-μm thickness, and stained with hematoxylin and eosin (HE). To evaluate and quantify goblet cells, sections were stained with Alcian Blue/Periodic Acid–Schiff (AB/PAS). Deparaffinized and rehydrated tissue slides were stained with 3% acetic acid for 3 min, followed by Alcian Blue for 30 min, 0.5% periodic acid for 5 min, and then Schiff Reagent for 10 min.

### 2.3. Immunohistochemistry (IHC)

The following primary antibodies were used for evaluating small intestinal restitution: monoclonal mouse anti-E-cadherin (Thermo Fisher Scientific, Carlsbad, CA, USA); monoclonal mouse anti-vimentin (Dako, Glostrup, Denmark); polyclonal rabbit anti-Snail (Biorbyt, San Francisco, CA, USA); polyclonal rabbit anti-ZO-1/TJP1 (Thermo Fisher Scientific, Carlsbad, CA, USA); monoclonal mouse anti-actin (Thermo Fisher Scientific, CA, USA); monoclonal mouse anti-human Ki-67 (Dako, Carpinteria, CA, USA); and monoclonal mouse anti-cytokeratin peptide 18 (Sigma-Aldrich, St. Louis, MO, USA). Specificity of these antibodies for swine tissue has been validated (Chen et al., 2020; Jung et al., 2015a; Ladel et al., 2019; Vermeulen et al., 2018; Palmieri et al., 2011).

Immunohistochemistry was performed at the Iowa State University Veterinary Diagnostic Laboratory (Ames, IA, USA). Sections of the jejunum and ileum were placed onto Superfrost® Plus slides (VWR™, Radnor, PA, USA) and dried in a 60 °C oven for 20 min prior to the automated staining process. One of two research platforms were used to complete each automated IHC protocol from deparaffinization through the staining process: 1) Roche Ventana Medical Systems DISCOVERY ULTRA and 2) Leica Biosystems BOND RX. Ready-to-use ancillary and detection reagents from Ventana (Ventana Medical Systems, Inc., Tucson, AZ) and Leica (Leica Biosystems, Inc. Buffalo Grove, IL, USA and Leica Biosystems, Newcastle, UK) were applied to each described protocol unless otherwise noted.

For IHC stains performed on the DISCOVERY ULTRA, tissue sections were first: deparaffinized with EZPrep solution, incubated with Cell Conditioning 1 (CC1) at 100 °C for 48 min and inhibited with Inhibitor ChromoMap (CM) for 8 min. Primary antibody application and incubation then occurred at the specific dilution ratio, time and temperature accordingly (E-cadherin, 1:200, 32 min, 37 °C; ZO-1,1:200, 40 min, 37 °C; actin, 1:200, 32 min, 37 °C; vimentin, 1:500, 32 min, 37 °C; Snail, 1:1000, 60 min, 37 °C; anti-cytokeratin 18, 1:1000, 32 min, 37 °C). DISCOVERY OmniMap anti-Rb HRP was applied for 16 min after the ZO-1 or Snail antibody incubation period. DISCOVERY OmniMap anti-Ms HRP was applied for 16 min after the actin, E-cadherin, vimentin or anti-cytokeratin antibody incubation period. Unique to the Snail IHC protocol was the addition of an amplification step. The DISCOVERY Amp HQ Kit was co-incubated for 20 min alongside the DISCOVERY Amplification anti-HQ HRP Multimer at 12 min. Chromogenic detection was finally accomplished using the DISCOVERY ChromoMap DAB Kit (RUO) by selecting DAB for each antibody followed by an 8 min Hematoxylin and 4 min Bluing incubation period on the instrument. Slides were next removed from the instrument, rinsed in soapy water and tap water to remove the liquid coverslip layer, dehydrated through a series of alcohols and xylene changes, mounted and coverslipped. The dehydration and coverslipping process was moved through an automated process on the Sakura Tissue-Tek® Prisma® slide stainer and Sakura Tissue-Tek® Glas™ gG coverslipper.

For the IHC stain performed on the Leica BOND RX, tissues were first deparaffinized with Bond Dewax Solution. The antigen was retrieved with BOND Epitope Retrieval Solution 2 for 20 min at 100 °C. Sections were subsequently treated with Peroxide Block from the BOND Intense R Detection kit for 5 min and blocked with an application of 10% Normal Goat Serum (MP Biomedicals, Solon, OH, USA) for 10 min. The primary antibody application and incubation then occurred at the specific dilution ratio, time and temperature accordingly (anti-human Ki-67, 1:250, 60 min, ambient). A Biotinylated Link (Dako North America, Inc., Carpinteria, CA, USA) was applied for 8 min before an additional 8 min incubation of Streptavidin-HRP from the BOND Intense R Detection kit. Detection was completed on the instrument using DAB Intense for 5 min and a hematoxylin incubation for 5 min. Slides were removed and immediately place on the automated stainer for dehydration before being coverslipped as previously described.

### 2.4. RNAscope® duplex chromogenic in situ hybridization (ISH) assay

For investigating the RNA levels of E-cadherin and N-cadherin, custom RNAscope® probes were designed by Advanced Cell Diagnostics (Advanced Cell Diagnostics, Newark, CA, USA). Two probes, CDH1 (cat. #843851) and CDH2 (cat. #843861-C2), were used for E-cadherin and N-cadherin, respectively. Tissue sections of jejunum and ileum were mounted on SuperFrost® Plus glass slides (VWR™, Radnor, PA, USA). Chromogenic ISH was performed at the Iowa State University Veterinary

Diagnostic Laboratory (Ames, IA, USA) using RNAscope® 2.5 HD Duplex Kit (Advanced Cell Diagnostics, Newark, CA, USA) with the procedure as instructed by the manufacturer.

### 2.5. Image analysis

All jejunum and ileum HE, AB/PAS, IHC, and ISH sections were examined with an Olympus BX40 microscope (Olympus Optical, Tokyo, Japan) equipped with an Olympus DP26 camera and CellSens Standard software (Olympus Optical, Tokyo, Japan). Lengths of 10 normally oriented villi and depths of associated crypts in jejunum and ileum were measured, and the average measurement units were presented as jejunal and ileal VH:CD ratios per pig.

To evaluate the cellular density of vimentin-positive enterocytes, vimentin immunopositive cells were counted throughout villi. The length of basement membrane of villi was measured by CellSens Standard software and presented as the epithelial length. In each pig, results were presented as numbers of vimentin immunopositive cells per μm length of epithelium in jejunum and in ileum, respectively. To evaluate cellular density of M cells, CK18 immunopositive cells were classified as villus M cells on villus epithelium in the jejunum and ileum, and Peyer's patch M cells on dome epithelium in the ileum. The numbers of villus M cells and Peyer's patch M cells were counted separately throughout tissue sections and presented as numbers per μm length of villus epithelium and follicle-associated epithelium, respectively.

For semi-quantitation of AB/PAS stain, IHC for Ki67, E-cadherin, Snail, actin, and ZO-1, as well as ISH for E-cadherin and N-cadherin, four images collected per jejunum or ileum per pig were captured using a 40X objective. Images of AB/PAS stain and IHC were analyzed semi-quantitatively using the Area Quantification module v1.0 within the HALO image analysis platform (v2.0.1145.19, Indica Labs, Corrales, NM, USA), while images of ISH were analyzed semi-quantitatively using the in-situ hybridization module within the HALO image analysis platform.

For AB/PAS stain, the whole layer of mucosa in the captured images was manually selected, and AB/PAS-stained signal in the region of interest was quantified. In each pig, results were presented as mean values of AB/PAS-stained area ($\mu m^2$) per μm length of epithelium in jejunum and ileum, respectively. For the IHC for Ki67, crypts in captured images were manually selected, and the DAB chromogen deposition in the region of interest was quantified. In each pig, results were presented as mean values of Ki67 immunopositive area ($\mu m^2$) per μm length of epithelium in jejunum and ileum, respectively.

To evaluate EMT of villus tips, the IHC for E-cadherin, Snail, actin, and ZO-1, as well as ISH for E-cadherin and N-cadherin were evaluated only in the villus tips (Fig. 1). At least 10 villus tips which are well-orientated and lined by a single layer of epithelial cells in captured images were manually selected. IHC staining of E-cadherin, Snail, actin, and ZO-1 in the region of interest was quantified separately. In each pig, results were presented as mean immunopositive areas ($\mu m^2$) per μm length of epithelium in jejunum and ileum, respectively. ISH for E-cadherin and N-cadherin was quantified, and results were presented as mean E-cadherin-positive or N-cadherin-positive areas ($\mu m^2$) per cell area ($\mu m^2$) in jejunum and ileum, respectively.

### 2.6. Protein quantification assay

To evaluate the expression of intestinal cytokine and metalloproteinases (MMP) during restitution, jejunum from pigs at DPI 10 was collected as described above. Frozen jejunum tissues were homogenized in PBS buffer (50 mM HEPES, 150 mM NaCl, 50 mM NaF, 2 mM EDTA, 5% glycerol, 1% Triton X, 0.1% protease inhibitor cocktail) and centrifuged at 2000×*g* for 10 min at 4 °C. The supernatant was collected, and protein concentrations were determined via a Pierce bicinchoninic acid (BCA) assay (Thermofisher Scientific, Carlsbad, CA, USA). Using commercial ELISA kits, transforming growth factor (TGF)-β1 (MB100B, R&D Systems, Minneapolis, MN, USA), interleukin (IL)-17 (ABIN415866, Antibodies-online Inc., Atlanta, GA, USA), and MMP 9 (ABIN431284, Antibodies-online Inc., Atlanta, GA, USA), according to the manufacturer's instructions, respectively.

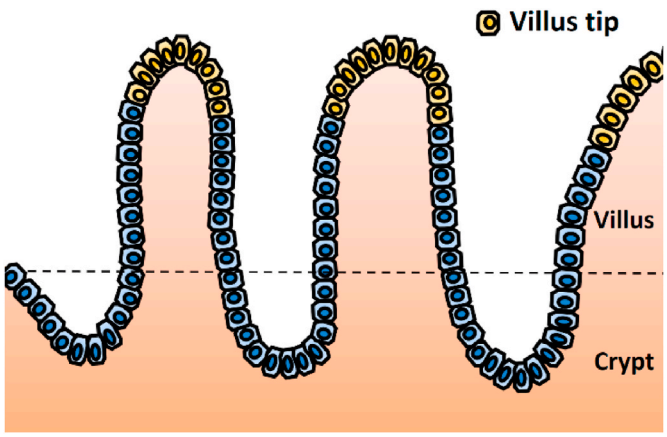


**Fig. 1.** Diagram of the anatomical divisions in small intestinal mucosa. To investigate epithelial-mesenchymal transition, immunohistochemistry for E-cadherin, Snail, actin, and ZO-1, as well as in situ hybridization for E-cadherin and N-cadherin, were evaluated only in the villus tip area (highlighted as yellow cells in the diagram). The image analysis was performed on the HALO image analysis platform.

### 2.7. Statistical analysis

All data were analyzed using JMP® software 15 (SAS Inst. Inc., Cary, NC, USA), and each pig was considered as an experimental unit. Non-parametric statistical tests, such as the Wilcoxon rank sum test and Spearman's rank-ordered correlation, were performed on results of IHC, ISH, and protein quantification assay. A p-value $\leq 0.05$ was considered as a significant difference.

## 3. Results

### 3.1. EMT at villus tips occurs in the jejunum

To verify the hypothesis that PEDV infection results in EMT in enterocytes at the villus tips, the antigens of E-cadherin, vimentin, Snail were evaluated via IHC. Results of IHC showed that E-cadherin was expressed in the cytoplasm of enterocytes, particularly at the lateral surface, while Snail as a transcription factor was mainly expressed in the nuclei of enterocytes. Sporadically, there were enterocytes that contained intracytoplasmic vimentin protein scattered along the villi. Due to a low number of vimentin-positive cells, the result was presented as cellular density instead of semi-quantification applied for E-cadherin and Snail expression. The jejunum of PEDV-infected pigs had a reduced expression of E-cadherin ($P = 0.020$) but an increased expression of Snail ($P = 0.011$), with more vimentin-positive cells compared to the controls ($P = 0.045$; Fig. 2). Furthermore, in the jejunum of the PEDV-infected pigs, E-cadherin expression was negatively correlated with the number of vimentin-positive cells ($R = -0.548$, $P = 0.012$) and Snail expression ($R = -0.554$, $P = 0.035$), but positively correlated with VH:CD ratio ($R = 0.658$, $P = 0.014$). In the ileum, on the other hand, neither expression of E-cadherin and Snail nor the number of vimentin-positive cells had a significant difference between controls and PEDV-infected pigs.

### 3.2. RNA expression of N-cadherin increased in the jejunum

To further study EMT in enterocytes, we measured RNA abundance of E-cadherin and N-cadherin via ISH. In both jejunum and ileum, RNA

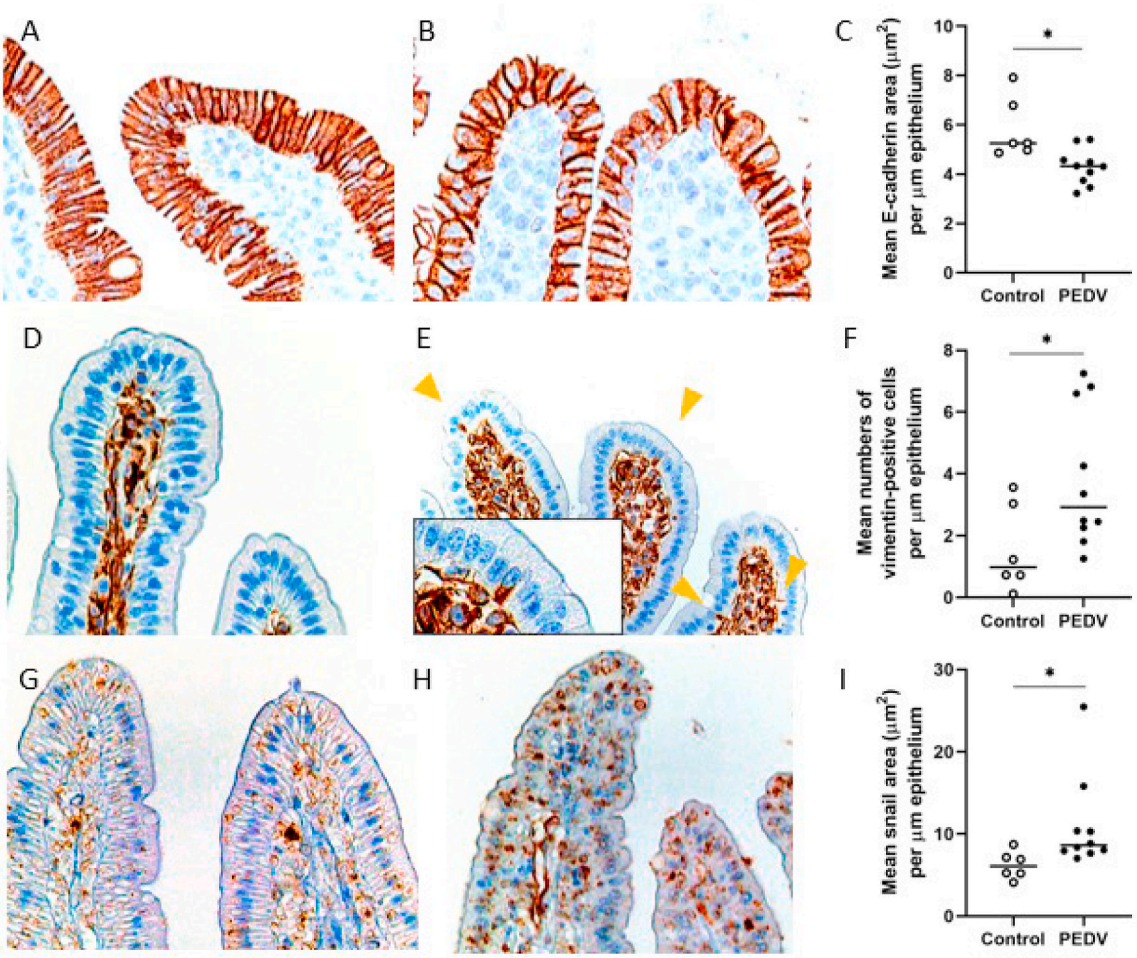


**Fig. 2.** Epithelial-mesenchymal transition at the villus tips in the jejunum after PEDV infection. (A–B) E-cadherin antigens in a control pig (A) and a PEDV-infected pig (B). Immunohistochemistry (IHC) for E-cadherin. (C) The mean values of E-cadherin immunopositive area ($\mu m^2$)/μm length of epithelium. (D–E) Vimentin antigens in a control pig (D) and a PEDV-infected pig (E). Arrowheads indicate vimentin antigen in enterocytes. Insert: a higher magnification of enterocytes. IHC for vimentin. (F) The mean numbers of vimentin-positive enterocytes/μm of epithelium. (G–H) Snail antigens in a control pig (G) and a PEDV-infected pig (H). IHC for Snail. (I) The mean values of Snail immunopositive area ($\mu m^2$)/μm length of epithelium. Bars show the mean values for each group, including the control (n = 6, open dots) and PEDV (n = 10, closed dots) treatments. * indicates a significant difference ($P < 0.05$).

of E-cadherin was mainly expressed in the apical cytoplasm of enterocytes, which is a similar location as E-cadherin protein. Unlike E-cadherin, N-cadherin was expressed in the nuclei of enterocytes. In comparison to controls, the RNA abundance of N-cadherin in the jejunum of PEDV pigs increased ($P = 0.042$) (Fig. 3). However, no significant differences were detected in RNA abundance of N-cadherin in the ileum or E-cadherin in both jejunum and ileum between controls and PEDV-infected pigs.

### 3.3. Impairment of tight junctions and microvilli in the jejunum

We next verified structural components in enterocytes, including ZO-1 and actin as critical proteins for constructing tight junction complexes and microvilli, respectively. Results of IHC showed that actin antigen was present at the apical surface of enterocytes, which is the same location as the microvilli. Compared to villus enterocytes, enterocytes in the crypts showed negative or weak actin presence. On the other hand, ZO-1 antigen was expressed at the lateral aspects near the apical surface of enterocytes forming a delicate meshwork pattern, which is consistent with the tight junctions. In comparison to controls, the jejunum in PEDV pigs had decreased expressions of ZO-1 ($P = 0.045$) and actin ($P = 0.026$) (Fig. 4). Additionally, expression of both proteins was positively correlated with E-cadherin expression ($R = 0.656$ and 0.509, $P = 0.006$ and 0.044, respectively) and negatively correlated with the number of vimentin-positive cells ($R = -0.500$, $P < 0.05$, all analyses).

### 3.4. Increased TGFβ1 concentration in the jejunum

Having demonstrated EMT in the jejunum, we were interested in possible factors attributed to EMT and the changes in metalloproteinases. TGFβ1, IL-17, and MMP9 were evaluated by ELISA. Jejunum tissue homogenates from PEDV-infected pigs had a significantly increased TGFβ1 protein concentration when compared to controls ($P = 0.034$; Fig. 5). However, IL-17 and MMP 9 protein concentrations were undetectable in both controls and PEDV-infected pigs by ELISA (Data not shown).

### 3.5. Reduced Peyer's patch M cells in the ileum

To study the restitution of different enterocyte subtypes after PEDV infection, we evaluated the VH:CD ratio, the expression of mucin in goblet cells, the activity of stem cells, and the cellular density of villous M cells and Peyer's patch M cells. PEDV-infected pigs had decreased numbers of Peyer's patch M cells on the follicle-associated epithelium of ileum when compared to controls ($P = 0.045$; Fig. 6). There was no significant difference in VH:CD ratio, expression of mucin in goblet cells,

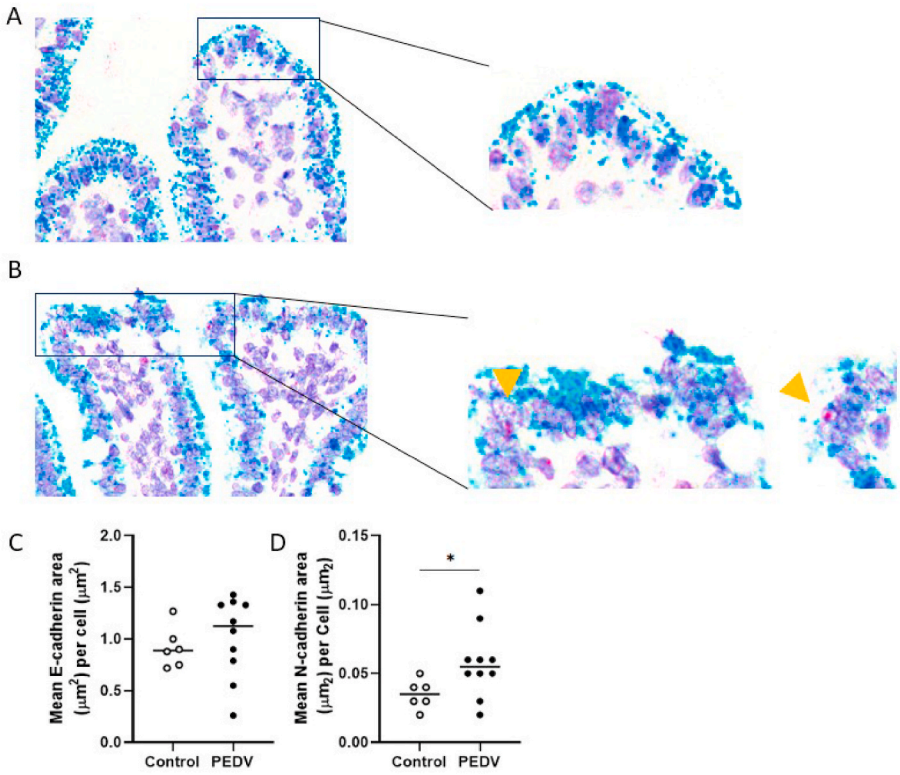


**Fig. 3.** Increased RNA level of N-cadherin at the villus tips in the jejunum after PEDV infection. (A) RNA of E-cadherin (green) in a control pig. *In situ* hybridization (ISH) for E-cadherin and N-cadherin. (B) RNA of E-cadherin (green) and RNA of N-cadherin (red) in a PEDV-infected pig. Arrowheads indicate N-cadherin RNA in enterocytes. ISH for E-cadherin and N-cadherin. (C) Mean values of E-cadherin-positive area ($\mu m^2$)/cell area ($\mu m^2$). (D) Mean values of N-cadherin-positive area ($\mu m^2$)/cell area ($\mu m^2$). Bars show the mean values for each group, including the control (n = 6, open dots) and PEDV (n = 10, closed dots) treatments. * indicates a significant difference ($P < 0.05$).

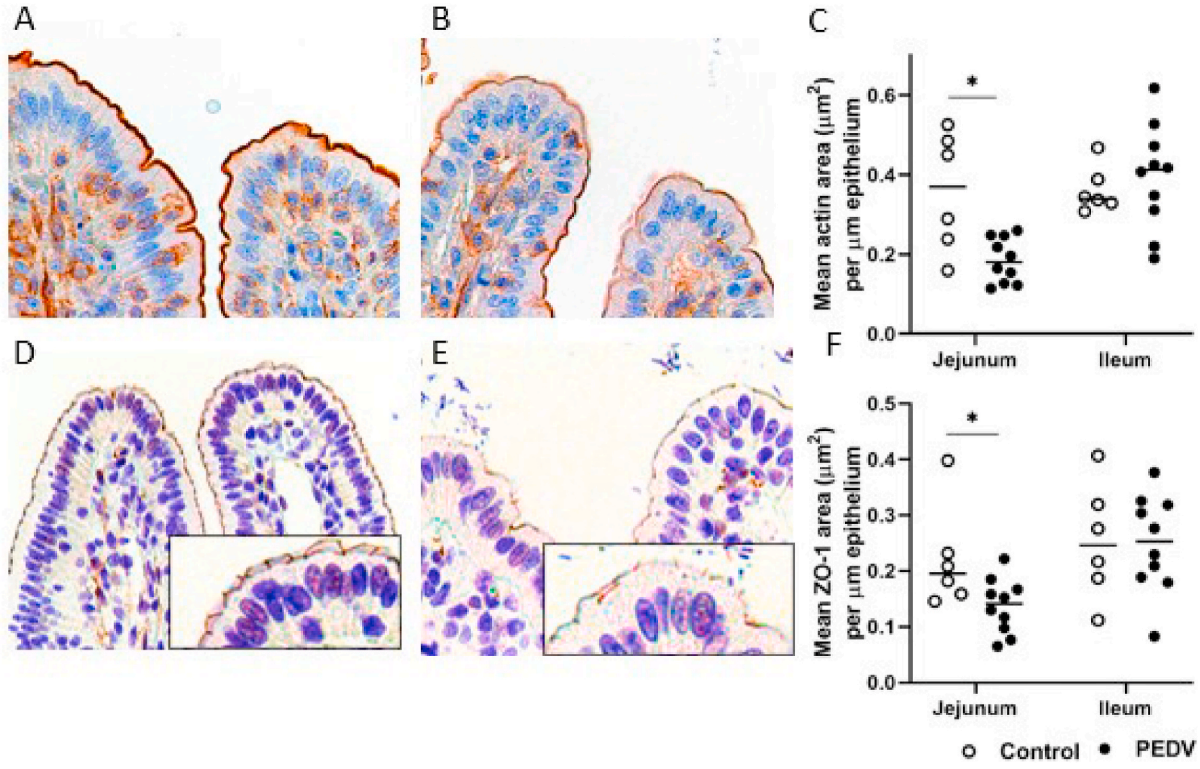


**Fig. 4.** Impairment of tight junctions and microvilli in the jejunum after PEDV infection. (A–B) Actin antigens in a control pig (A) and a PEDV-infected pig (B). Immunohistochemistry (IHC) for actin. (C) The mean values of actin immunopositive area ($\mu m^2$)/μm length of epithelium. (D–E) ZO-1 antigens in a control pig (D) and a PEDV pig (E). Insert: a higher magnification of enterocytes. IHC for ZO-1. (F) The mean values of ZO-1 immunopositive area ($\mu m^2$)/μm length of epithelium. Bars show the mean values for each group, including the control (n = 6, open dots) and PEDV (n = 10, closed dots) treatments. * indicates a significant difference ($P < 0.05$).

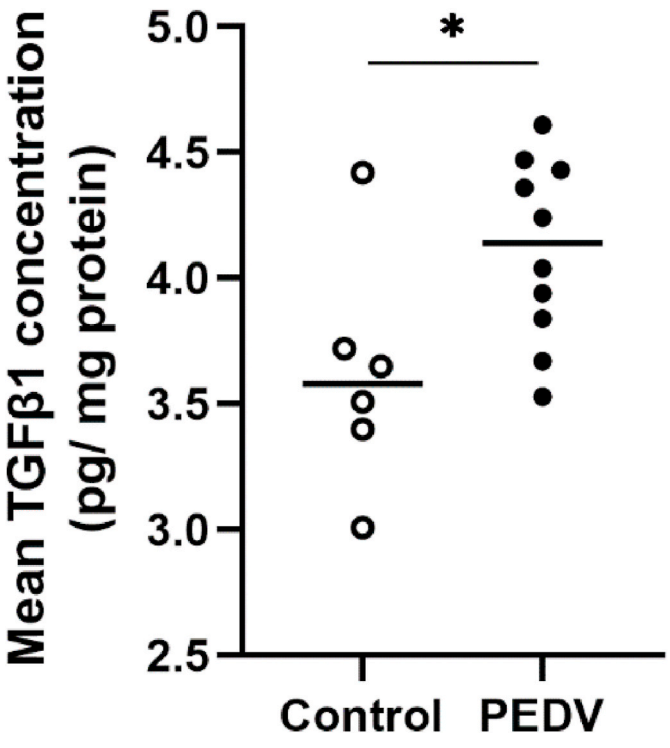


**Fig. 5.** The mean values of TGFβ1 protein concentration in the jejunum of control and PEDV-infected pigs after PEDV infection. Bars show the mean values for each group, including the control (n = 6, open dots) and PEDV (n = 10, closed dots) treatments. * indicates a significant difference ($P < 0.05$).

activity of stem cells, and cellular density of villous M cells in both jejunum and ileum between controls and PEDV-infected pigs (Fig. 6).

## 4. Discussion

Epithelial-mesenchymal transition (EMT) is a process in which epithelial cells lose polarity and convert into a motile mesenchymal phenotype. EMT is not only indispensable in the development of most organs and wound healing but also pathologically contributes to fibrosis and tumor progression (Chen et al., 2016b). In general, when cells undergo injuries, such as viral infection, endoplasmic reticulum (ER) stress is stimulated via different mechanisms (Malhotra and Kaufman, 2007). Following injuries, the amount of unfolding protein in the endoplasmic reticulum is increased and subsequently stimulates unfolded protein response (UPR) and autophagy to accommodate, which is termed acute ER stress (Rao et al., 2004). Acute ER stress had been found in different coronavirus diseases, including PEDV infection, due to the disruption of cellular homeostasis by double-membrane vesicles (DMVs) formation in the cytoplasm, which is required for viral replication (Fung et al., 2014; Xu et al., 2013). These burdened cells might undergo apoptosis or turn into chronic ER stress (Li, 2018). At the chronic stage, TGFβ is produced by these stressed cells or activated inflammatory cells and leads to EMT in surviving cells (Johno and Kitamura, 2013). Additionally, increased TGFβ is usually observed in the late stage of inflammation as a critical factor in tissue repairment (Wang et al., 2006). In humans, EMT in the digestive tract is well known in inflammatory bowel disease (IBD) which is highly associated with chronic inflammation (Gassler et al., 2001; Zidar et al., 2016). These findings indicate that EMT is a relatively chronic response to injury. Chronic inflammation induced by bacterial infections could lead to EMT in the intestinal epithelium (Hofman and Vouret-Craviari, 2012). To examine intestinal restitution and the possibility of EMT after PEDV infection, we focused on pigs at DPI 10. Herein, we demonstrated EMT at villus tips in the jejunum of weaned pigs 10 days after PEDV infection. In these pigs, EMT was characterized by a localized concurrence of reduced E-cadherin protein abundance, increased protein abundance of vimentin, as well as elevated localized RNA abundance of N-cadherin. Additionally, there was a negative correlation between E-cadherin and vimentin expressions in these samples. These findings indicate the switch between epithelial and mesenchymal phenotypes in intestinal epithelial cells. Interestingly, the gene abundance of E-cadherin was not different between the control and PEDV treatments. It is suspected that at the beginning of EMT, the gene abundance of the E-cadherin is reduced which leads to a subsequent reduction of E-cadherin protein (Lamouille et al., 2014). However, herein the mRNA abundance of E-cadherin appeared to be restored by DPI 10.

To further elucidate to the mechanisms involved in the PEDV-induced EMT, the transcription factor and regulatory signaling pathways were investigated. Switches in intestinal epithelial cell differentiation are triggered by several key transcription factors including Snail, TWIST, and zinc-finger E-box-binding (ZEB) (Lamouille et al., 2014). In addition, it has been shown that pro-inflammatory cytokines, including TGFβ family and IL-17, activates Snail expression leading to EMT (Zhang et al., 2018; Nisticò et al., 2012). In pigs, TGFβ induces EMT in thyroid and intestinal epithelial cells through a MEK-dependent mechanism (Xia et al., 2017; Grände et al., 2002). Herein, we observed an increase in Snail expression in the jejunum and ileum. This was negatively correlated with the expression of E-cadherin, but positively correlated with the number of vimentin-positive epithelial cells. These data suggest that the Snail transcription factor plays a role in EMT post-PEDV infection in pigs. We have also observed an increased protein concentration of TGFβ1 in the jejunum at DPI 10 in the PEDV treatment, suggesting that the Snail transcription factor is activated by TGFβ1 as previously reported (Zhang et al., 2018; Nisticò et al., 2012). Interestingly, we were unable to detect any IL-17 protein in our jejunum tissue homogenates. This may be a result of the ELISA not being sensitive enough to detect the protein in our homogenate, or IL-17 might not be a key contributor in PEDV-induced EMT.

Rearranged cell membrane and reorganized microfilaments resulting from PEDV replication has been identified *in vivo* (Zhou et al., 2017; Zhao et al., 2014). Decreased gene and protein abundance of tight junction proteins have been reported in nursing piglets and weaned pigs during PEDV infection (Jung et al., 2015a; Schweer et al., 2016; Curry et al., 2017b; Zong et al., 2019). These findings indicate that PEDV infection leads to impaired intestinal integrity via altered tight junction assembly. In support of this, in the present study we demonstrated the reduction of actin and ZO-1 in microvilli and tight junctions, respectively. Additionally, localized actin and ZO-1 protein abundance were positively correlated with E-cadherin protein abundance and negatively correlated with the number of vimentin-positive cells. These data suggest an association between EMT and disruption of microvilli and tight junctions. The microvilli located on the apical surface of absorptive enterocytes, constructed by actin filaments and various actin-binding proteins, increase the surface area of the digestive tract (Fath and Burgess, 1995; Bretscher and Weber, 1978; Hagen and Trier, 1988). At the basolateral surface, the tight junctions are the most apical intercellular junction, which limits paracellular flux. Zonula occludens-1 (ZO-1) in tight junction complexes is a peripheral membrane protein with multiple connecting sites and forms a link between tight junctions and cytoskeleton for supporting protein-protein interactions (Shen et al., 2011; Fanning et al., 1998). Collectively, microvilli and tight junctions are closely linked to the organization of actin cytoskeleton. EMT and TGFβ could rearrange the actin cytoskeleton organization and disassemble tight junctions, which disturbs the apical–basolateral polarization of epithelial cells (Thiery and Sleeman, 2006; Ozdamar et al., 2005). It is therefore speculated that the microvillus blunting and disrupted tight junction of the intestinal epithelium observed in PEDV-infected pigs in the present study is the sequela of disarrangement of cytoskeleton caused by both EMT and TGFβ up-regulation.

Given these parameters, although the jejunal VH:CD ratio appeared

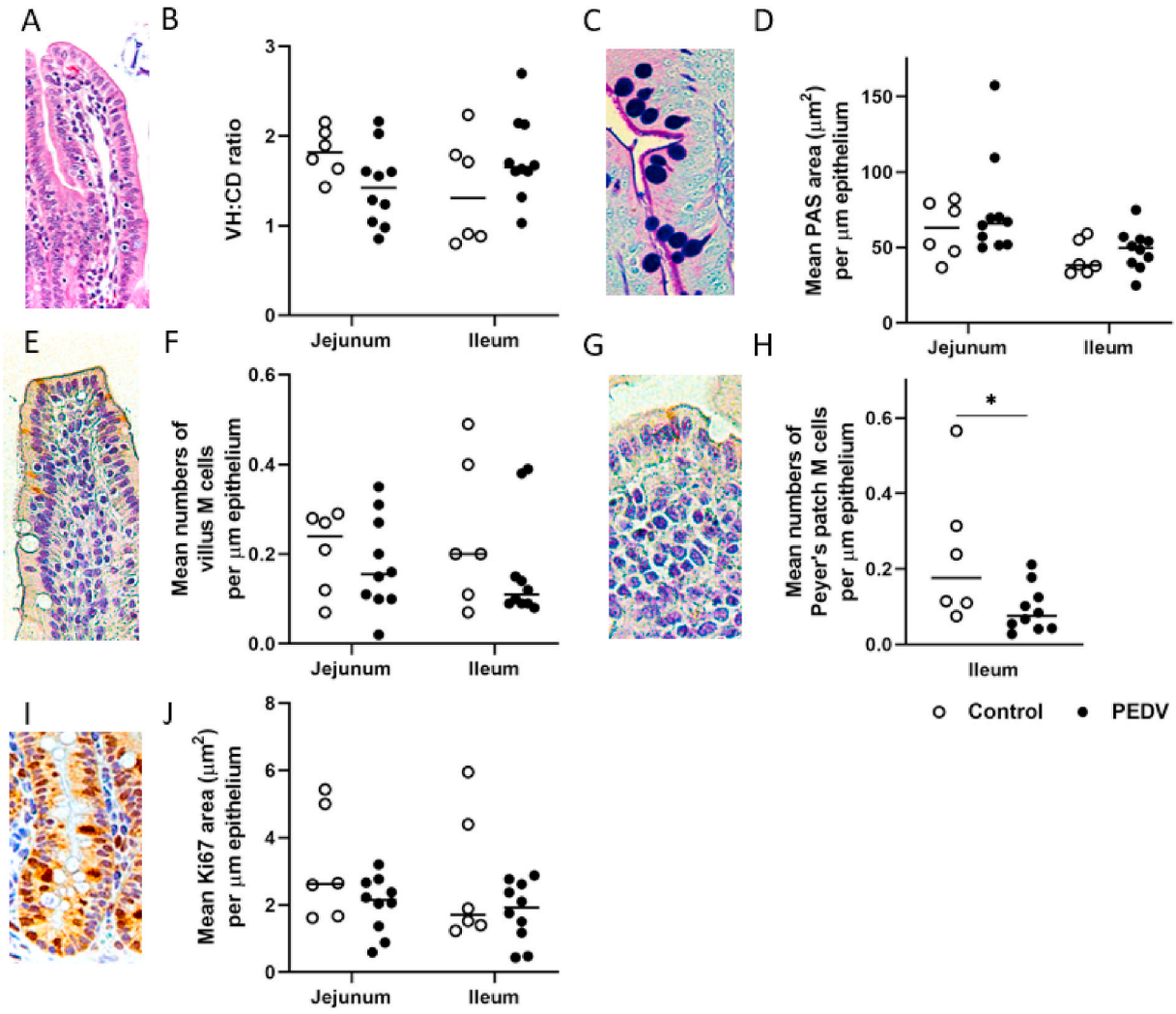


**Fig. 6.** Intestinal restitution in the jejunum and ileum after PEDV infection. (A) Restored intestinal villi in the jejunum. PEDV-infected pig. Hematoxylin and eosin stain. (B) The mean ratios of villus length to crypt depth (VH:CD) in the jejunum and ileum in controls and PEDV-infected pigs. (C) Goblet cells in the jejunal mucosa. PEDV-infected pig. Alcian Blue/Periodic Acid–Schiff (AB/PAS) stain. (D) The mean AB/PAS-stained areas ($\mu m^2$)/μm length of epithelium in the jejunum and ileum in controls and PEDV-infected pigs. (E) Villus M cells in the jejunal villi. PEDV-infected pig. Immunohistochemistry (IHC) for cytokeratin 18 (CK18). (F) The mean numbers of villus M cells/μm length of epithelium in the jejunum and ileum in controls and PEDV-infected pigs. (G) Peyer's patch M cells in the dome epithelium of the ileum. PEDV-infected pig. IHC for CK18. (H) The mean numbers of Peyer's patch M cells/μm length of epithelium in the jejunum and ileum in controls and PEDV-infected pigs. (I) Stem cell proliferation in the jejunal crypts. PEDV-infected pig. IHC for Ki67. (J) The mean Ki67-stained areas ($\mu m^2$)/μm length of epithelium in jejunum and ileum in controls and PEDV-infected pigs. Bars show the mean values for each group, including the control (n = 6, open dots) and PEDV (n = 10, closed dots) treatments. * indicates a significant difference ($P < 0.05$).

to be restored in PEDV-infected pigs at DPI 10, epithelial enterocytes at the villus tips displayed EMT as well as disrupted microvilli and tight junctions. Repair of the intestinal epithelium functionally and structurally depends on the cytoskeleton of cells (Albers et al., 1996). Additionally, disorganized microvilli decrease the total absorptive surface area in the small intestine, contributing to poor growth performance (Mosenthin, 1998). In PEDV-infected weaned pigs, reduction in ADG and ADFI was observed, and the mechanisms of growth retardation was unclear (Curry et al., 2017a; Schweer et al., 2016). Therefore, it is suggested that the impeded growth performance might be associated with incomplete restitution of epithelial cells. Interestingly, these post-infection alterations in villus tips were observed in jejunum but not in the ileum. Based on our previous study (Chen et al., 2020), PEDV infection resulted in decreased VH:CD ratios in jejunum on DPI 2, 4, and 6 and in ileum on DPI 4 only, and the results indicate that jejunum had more severe villus injury than ileum. Moreover, in the present study, a positive correlation was observed between the E-cadherin expression and VH:CD ratio. Therefore, it is suspected that PEDV-induced EMT in jejunum persisting to at least 10 days after viral infection is associated with a more severe impairment in the jejunum.

Epithelial restitution in the small intestine relies on the differentiation of stem cells in crypts into specialized epithelial cells along the crypt-villus axis (van derFlier and Clevers, 2009). Depletion of goblet cells at DPI 3 and 5 and increased stem cell proliferation at DPI 5 and 7 were observed in weaned pigs during PEDV infection (Jung and Saif, 2017; Jung et al., 2015b). Contrary to these findings, our data showed no difference of either PAS expressing goblet cells or Ki67 expression in stem cells between control and PEDV treatment groups at DPI 10. These discrepancies may be related to age, viral strain, and experimental time points. It has been reported in PEDV challenged pigs that jejunum stem cell proliferation (Ki67 expressing cells) was similar to control naïve pigs by DPI 20 (Curry et al., 2018). Altogether, these results suggest a complete restitution of goblet cells and no significant changes in stem cell proliferation at 10 days after PEDV infection.

As antigen delivering cells, M cells are able to engulf and deliver luminal antigens to underlying immune cells. Based on the location, M

cells in the small intestine are divided into villus M cells and Peyer's patch M cells. Villus M cells are scattered among the absorptive enterocytes on the villi, whereas Peyer's patch M cells are located on the dome epithelium above the Peyer's patch. Moreover, villus M cells are mainly inducible from enterocyte trans-differentiation, while Peyer's patch M cells are constitutively derived from stem cells (Lo, 2018). We have previous reported that, during PEDV infection, induction of Peyer's patch M cells at DPI 2 was followed by a reduction at DPI 6 when the ileal VH:CD ration has been restored. Herein, a reduction of Peyer's patch M cells at DPI 10 was observed, when PEDV antigen was no longer detectable in the PEDV-infected pigs. The reduction indicates that M cells have a prolonged impairment due to PEDV infection. To our knowledge, this is the first report where the number of Peyer's patch M cells are diminished after viral infection. Due to the unique distribution, Peyer's patch M cells frequently form M cell-dendritic cell (DC) functional units and have high interaction with immune cells (Wang et al., 2011). Moreover, M cell-targeting vaccines are considered as an effective and promising immune strategy (Du et al., 2018; Jiang et al., 2014; Dhakal and Renukaradhya, 2019). Together, these findings suggest that the depletion of Peyer's patch M cells possibly results in an undermined immune surveillance in the small intestine that may reduce the efficiency of mucosal vaccines in weaned pigs recently infected with PEDV and further investigation into this possibility is warranted.

The mechanism of the reduction of Peyer's patch M cell is unclear, and it might be related to activity of stem cells, factors that mediate M cell differentiation from stem cells, or direct injury to M cells. Several factors, including but not limiting to lymphotoxin, TNFα, and RANKL, mediate the differentiation of Peyer's patch M cells from stem cells (Knoop et al., 2009; Wang et al., 2009; deLau et al., 2012). In addition, gut-innervating nociceptor suppresses the density of M cells to limit the entry of pathogens, such as *Salmonella enterica* (Lai et al., 2020). As we observed no difference between treatments regarding stem cell proliferation, the deletion or malfunction of stem cells seems not to happen in PEDV disease. It is unclear which factor or factors drive the depletion of Peyer's patch M cells in PEDV infection. Further studies are therefore warranted to elucidate the cause.

A limitation of this study is one single day of evaluation. Since the EMT is assumed to be related to incomplete restitution and chronic inflammation, pigs 14 or even 21 days after PEDV inoculation would be worth further study as well as an evaluation of the duration of M cell reduction.

## 5. Conclusions

The study describes specific aspects of epithelial restitution following PEDV infection and provides insights into potential mechanisms that may impede growth performance and immune function even after apparent clinical recovery. Overall, weaned pigs have incomplete intestinal restitution at 10 days post PEDV infection, despite clinical recovery and restoration of the VH:CD ratio. Post-infection alterations include EMT, disassembled microvilli, and disrupted tight junctions in absorptive enterocytes at the villus tips in the jejunum. There is also a persistent reduction in Peyer's patch M cells in the ileum. These data further elucidate the host response to PEDV infection in weaned pigs and provide new knowledge regarding intestinal cell damage and subsequent restitution. Incomplete intestinal restitution could lead to impaired nutrient absorption and growth restriction, and suboptimal response to orally administered vaccines in pigs recently infected with PEDV.

## Funding

This project was supported by Agriculture and Food Research Initiative Competitive Grant AH 10072632017 from the USDA National Institute of Food and Agriculture (Blikslager, Gabler, Burrough, Odle).

## CRediT authorship contribution statement

**Ya-Mei Chen:** Conceptualization, Methodology, Software, Formal analysis, Investigation, Data curation, Writing - original draft, Visualization. **Emma T. Helm:** Validation, Investigation, Writing - review & editing. **Jennifer M. Groeltz-Thrush:** Methodology, Investigation, Writing - review & editing. **Nicholas K. Gabler:** Investigation, Resources, Writing - review & editing, Supervision, Project administration, Funding acquisition. **Eric R. Burrough:** Validation, Investigation, Resources, Writing - review & editing, Supervision, Project administration, Funding acquisition.

## Declaration of competing interest

The author(s) declare no potential conflicts of interest with respect to the research, authorship, and/or publication of this article.

## Acknowledgments

We thank members of the Livestock Infectious Disease Isolation Facility for their assistance and staff from the Iowa State University Veterinary Diagnostic Laboratory for slide preparation and technical assistance.

## References

Albers, T.M., Lomakina, I., Moore, R.P., 1996. Structural and functional roles of cytoskeletal proteins during repair of native Guinea pig intestinal epithelium. Cell Biol. Int. 20, 821–830.
Bretscher, A., Weber, K., 1978. Localization of actin and microfilament-associated proteins 1n the microvilli and terminal web of the intestinal brush border by immunofluorescence microscopy. J. Cell Biol. 79, 839–845.
Chen, Q., Gauger, P.C., Stafne, M.R., Thomas, J.T., Madson, D.M., Huang, H., Zheng, Y., Li, G., Zhang, J., 2016a. Pathogenesis comparison between the United States porcine epidemic diarrhoea virus prototype and S-INDEL-variant strains in conventional neonatal piglets. J. Gen. Virol. 97, 1107–1121.
Chen, X., Bode, A.M., Dong, Z., Cao, Y., 2016b. The epithelial-mesenchymal transition (EMT) is regulated by oncoviruses in cancer. Faseb. J. 30, 3001–3010.
Chen, Y.-M., Helm, E., Gabler, N., Hostetter, J., Burrough, E., 2020. Alterations in intestinal innate mucosal immunity of weaned pigs during porcine epidemic diarrhea virus infection. Vet. Pathol. 57, 642–652.
Council, N.R., 2012. Nutrient Requirements of Swine: Eleventh Revised Edition. The National Academies Press, Washington, DC.
Curry, S.M., Gibson, K.A., Burrough, E.R., Schwartz, K.J., Yoon, K.J., Gabler, N.K., 2017a. Nursery pig growth performance and tissue accretion modulation due to porcine epidemic diarrhea virus or porcine deltacoronavirus challenge. J. Anim. Sci. 95, 173–181.
Curry, S.M., Schwartz, K.J., Yoon, K.J., Gabler, N.K., Burrough, E.R., 2017b. Effects of porcine epidemic diarrhea virus infection on nursery pig intestinal function and barrier integrity. Vet. Microbiol. 211, 58–66.
Curry, S.M., Burrough, E.R., Schwartz, K.J., Yoon, K.J., Lonergan, S.M., Gabler, N.K., 2018. Porcine epidemic diarrhea virus reduces feed efficiency in nursery pigs. J. Anim. Sci. 96, 85–97.
Debouck, P., Pensaert, M., Coussement, W., 1981. The pathogenesis of an enteric infection in pigs, experimentally induced by the coronavirus-like agent, CV 777. Vet. Microbiol. 6, 157–165.
deLau, W., Kujala, P., Schneeberger, K., Middendorp, S., Li, V.S.W., Barker, N., Martens, A., Hofhuis, F., DeKoter, R.P., Peters, P.J., Nieuwenhuis, E., Clevers, H., 2012. Peyer's Patch M Cells derived from Lgr5+ stem cells require SpiB and are induced by RankL in cultured "miniguts.". Mol. Cell Biol. 32, 3639–3647.
Dhakal, S., Renukaradhya, G.J., 2019. Nanoparticle-based vaccine development and evaluation against viral infections in pigs. Vet. Res. 50, 1–14.
Du, L., Yu, Z., Pang, F., Xu, X., Mao, A., Yuan, W., He, K., Li, B., 2018. Targeted delivery of GP5 antigen of PRRSV to M cells enhances the antigen-specific systemic and mucosal immune responses. Front. Cell Infect. Microbiol. 8, 1–10.
Eastham, A.M., Spencer, H., Soncin, F., Ritson, S., Merry, C.L.R., Stern, P.L., Ward, C.M., 2007. Epithelial-mesenchymal transition events during human embryonic stem cell differentiation. Canc. Res. 67, 11254–11262.
Fanning, A.S., Jameson, B.J., Jesaitis, L.A., Anderson, J.M., 1998. The tight junction protein ZO-1 establishes a link between the transmembrane protein occludin and the actin cytoskeleton. J. Biol. Chem. 273, 29745–29753.
Fath, K.R., Burgess, D.R., 1995. Microvillus assembly: not actin alone. Curr. Biol. 5, 591–593.
Fung, T.S., Huang, M., Liu, D.X., 2014. Coronavirus-induced ER stress response and its involvement in regulation of coronavirus-host interactions. Virus Res. 194, 110–123.
Gassler, N., Rohr, C., Schneider, A., Kartenbeck, J., Bach, A., Obermüller, N., Otto, H.F., Autschbach, F., 2001. Inflammatory bowel disease is associated with changes of enterocytic junctions. Am. J. Physiol. Gastrointest. Liver Physiol. 281, 216–228.

Grände, M., Å, Franzen, Karlsson, J.O., Ericson, L.E., Heldin, N.E., Nilsson, M., 2002. Transforming growth factor-β and epidermal growth factor synergistically stimulate epithelial to mesenchymal transition (EMT) through a MEK-dependent mechanism in primary cultured pig thyrocytes. J. Cell Sci. 115, 4227–4236.
Hagen, S.J., Trier, J.S., 1988. Immunocytochemical localization of actin in epithelial cells of rat small intestine by light and electron microscopy. J. Histochem. Cytochem. 36, 717–727.
Hofman, P., Vouret-Craviari, V., 2012. Microbes-induced EMT at the crossroad of inflammation and cancer. Gut Microb. 3, 176–185.
Jiang, T., Singh, B., Li, H.S., Kim, Y.K., Kang, S.K., Nah, J.W., Choi, Y.J., Cho, C.S., 2014. Targeted oral delivery of BmpB vaccine using porous PLGA microparticles coated with M cell homing peptide-coupled chitosan. Biomaterials 35, 2365–2373.
Johno, H., Kitamura, M., 2013. Pathological in situ reprogramming of somatic cells by the unfolded protein response. Am. J. Pathol. 183, 644–654.
Jung, K., Saif, L.J., 2017. Goblet cell depletion in small intestinal villous and crypt epithelium of conventional nursing and weaned pigs infected with porcine epidemic diarrhea virus. Res. Vet. Sci. 110, 12–15.
Jung, K., Eyerly, B., Annamalai, T., Lu, Z., Saif, L.J., 2015a. Structural alteration of tight and adherens junctions in villous and crypt epithelium of the small and large intestine of conventional nursing piglets infected with porcine epidemic diarrhea virus. Vet. Microbiol. 177, 373–378.
Jung, K., Annamalai, T., Lu, Z., Saif, L.J., 2015b. Comparative pathogenesis of US porcine epidemic diarrhea virus (PEDV) strain PC21A in conventional 9-day-old nursing piglets vs. 26-day-old weaned pigs. Vet. Microbiol. 178, 31–40.
Kim, Y., Lee, C., 2014. Porcine epidemic diarrhea virus induces caspase-independent apoptosis through activation of mitochondrial apoptosis-inducing factor. Virology 460–461, 180–193.
Knoop, K.A., Kumar, N., Butler, B.R., Sakthivel, S.K., Taylor, R.T., Nochi, T., Akiba, H., Yagita, H., Kiyono, H., Williams, I.R., 2009. RANKL is necessary and sufficient to initiate development of antigen-sampling M Cells in the intestinal epithelium. J. Immunol. 183, 5738–5747.
Koh, H.W., Kim, M.S., Lee, J.S., Kim, H., Park, S.J., 2015. Changes in the swine gut microbiota in response to porcine epidemic diarrhea infection. Microb. Environ. 30, 284–287.
Ladel, S., Schlossbauer, P., Flamm, J., Luksch, H., Mizaikoff, B., Schindowski, K., 2019. Improved in vitro model for intranasal mucosal drug delivery: primary olfactory and respiratory epithelial cells compared with the permanent nasal cell line RPMI 2650. Pharmaceutics 11, 367.
Lai, N.Y., Musser, M.A., Pinho-Ribeiro, F.A., Baral, P., Jacobson, A., Ma, P., Potts, D.E., Chen, Z., Paik, D., Soualhi, S., Yan, Y., Misra, A., Goldstein, K., Lagomarsino, V.N., Nordstrom, A., Sivanathan, K.N., Wallrapp, A., Kuchroo, V.K., Nowarski, R., Starnbach, M.N., Shi, H., Surana, N.K., An, D., Wu, C., Huh, J.R., Rao, M., Chiu, I.M., 2020. Gut-innervating nociceptor neurons regulate Peyer's Patch microfold cells and SFB levels to mediate Salmonella host defense. Cell 180 (33–49), e22.
Lamouille, S., Xu, J., Derynck, R., 2014. Molecular mechanisms of epithelial-mesenchymal transition. Nat. Rev. Mol. Cell Biol. 15, 178–196.
Li, C., 2018. The role of endoplasmic reticulum stress in the development of fibrosis in crohn's disease. Explor Res Hypothesis Med 3, 33–41.
Liu, S., Zhao, L., Zhai, Z., Zhao, W., Ding, J., Dai, R., Sun, T., Meng, H., 2015. Porcine epidemic diarrhea virus infection induced the unbalance of gut microbiota in piglets. Curr. Microbiol. 71, 643–649.
Lo, D.D., 2018. Vigilance or subversion? Constitutive and inducible M cells in mucosal tissues. Trends Immunol. 39, 185–195.
Malhotra, J.D., Kaufman, R.J., 2007. Endoplasmic reticulum stress and oxidative stress: a vicious cycle or a double-edged sword? Antioxidants Redox Signal. 9, 2277–2293.
Mosenthin, R., 1998. Physiology of small and large intestine of swine. AJAS (Asian-Australas. J. Anim. Sci.) 11, 608–619.
Niederwerder, M.C., Hesse, R.A., 2018. Swine enteric coronavirus disease: a review of 4 years with porcine epidemic diarrhoea virus and porcine deltacoronavirus in the United States and Canada. Transbound Emerg Dis 65, 660–675.
Nisticò, P., Bissell, M.J., Radisky, D.C., 2012. Epithelial-mesenchymal transition: general principles and pathological relevance with special emphasis on the role of matrix metalloproteinases. Cold Spring Harb Perspect Biol 4, 1–11.
Ozdamar, B., Bose, R., Barrios-Rodiles, M., Wang, H.R., Zhang, Y., Wrana, J.L., 2005. Regulation of the polarity protein Par6 by TGFβ receptors controls epithelial cell plasticity. Science 80 (307), 1603–1609.
Palmieri, G., Bergamo, P., Luini, A., Ruvo, M., Gogliettino, M., Langella, E., Saviano, M., Hegde, R.N., Sandomenico, A., Rossi, M., 2011. Acylpeptide hydrolase inhibition as targeted strategy to induce proteasomal down-regulation. PLoS One2011 e25888–e25888.
Rao, R.V., Ellerby, H.M., Bredesen, D.E., 2004. Coupling endoplasmic reticulum stress to the cell death program. Cell Death Differ. 11, 372–380.
Schweer, W.P., Pearce, S.C., Burrough, E.R., Schwartz, K., Yoon, K.J., Sparks, J.C., Gabler, N.K., 2016. The effect of porcine reproductive and respiratory syndrome virus and porcine epidemic diarrhea virus challenge on growing pigs II: intestinal integrity and function. J. Anim. Sci. 94, 523–532.
Shen, L., Weber, C.R., Raleigh, D.R., Yu, D., Turner, J.R., 2011. Tight junction pore and leak pathways: a dynamic duo. Annu. Rev. Physiol. 73, 283–309.
Tahoun, A., Mahajan, S., Paxton, E., Malterer, G., Donaldson, D.S., Wang, D., Tan, A., Gillespie, T.L., O'Shea, M., Roe, A.J., Shaw, D.J., Gally, D.L., Lengeling, A., Mabbott, N.A., Haas, J., Mahajan, A., 2012. Salmonella transforms follicle-associated epithelial cells into M cells to promote intestinal invasion. Cell Host Microbe 12, 645–656.
Thiery, J.P., Sleeman, J.P., 2006. Complex networks orchestrate epithelial-mesenchymal transitions. Nat. Rev. Mol. Cell Biol. 7, 131–142.
Thomas, J.T., Chen, Q., Gauger, P.C., Giménez-Lirola, L.G., Sinha, A., Harmon, K.M., Madson, D.M., Burrough, E.R., Magstadt, D.R., Salzbrenner, H.M., Welch, M.W., Yoon, K.J., Zimmerman, J.J., Zhang, J., 2015. Effect of porcine epidemic diarrhea virus infectious doses on infection outcomes in naïve conventional neonatal and weaned pigs. PloS One 10, 1–18.
Ullmann, U., In't Veld, P., Gilles, C., Sermon, K., DeRycke, M., Van deVelde, H., VanSteirteghem, A., Liebaers, I., 2007. Epithelial-mesenchymal transition process in human embryonic stem cells cultured in feeder-free conditions. Mol. Hum. Reprod. 13, 21–32.
van derFlier, L.G., Clevers, H., 2009. Stem cells, self-renewal, and differentiation in the intestinal epithelium. Annu. Rev. Physiol. 71, 241–260.
Vermeulen, M., DelVento, F., deMichele, F., Poels, J., Wyns, C., 2018. Development of a cytocompatible scaffold from pig immature testicular tissue allowing human sertoli cell attachment, proliferation and functionality. Int. J. Mol. Sci. 19.
Wang, X.J., Han, G., Owens, P., Siddiqui, Y., Li, A.G., 2006. Role of TGFβ-mediated inflammation in cutaneous wound healing. J. Invest. Dermatol. Symp. Proc. 11, 112–117.
Wang, J., Lopez-Fraga, M., Rynko, A., Lo, D.D., 2009. TNFR and LTβR agonists induce follicle-associated epithelium and M cell specific genes in rat and human intestinal epithelial cells. Cytokine 47, 69–76.
Wang, J., Gusti, V., Saraswati, A., Lo, D.D., 2011. Convergent and divergent development among M Cell lineages in mouse mucosal epithelium. J. Immunol. 187, 5277–5285.
Xia, L., Dai, L., Yu, Q., Yang, Q., 2017. Persistent transmissible gastroenteritis virus infection enhances enterotoxigenic Escherichia coli K88 adhesion by promoting epithelial-mesenchymal transition in intestinal epithelial cells. J. Virol. 91 e01256-17.
Xu, X.G., Zhang, H., Zhang, Q., Dong, J., Liang, Y., Huang, Y., Liu, H.J., Tong, D.W., 2013. Porcine epidemic diarrhea virus E protein causes endoplasmic reticulum stress and up-regulates interleukin-8 expression. Virol. J. 10, 26.
Zhang, H.J., Zhang, Y.N., Zhou, H., Guan, L., Li, Y., Sun, M.J., 2018. IL-17A promotes initiation and development of intestinal fibrosis through EMT. Dig. Dis. Sci. 63, 2898–2909.
Zhao, S., Gao, J., Zhu, L., Yang, Q., 2014. Transmissible gastroenteritis virus and porcine epidemic diarrhoea virus infection induces dramatic changes in the tight junctions and microfilaments of polarized IPEC-J2 cells. Virus Res. 192, 34–45.
Zhou, X., Cong, Y., Veenendaal, T., Klumperman, J., Shi, D., Mari, M., Reggiori, F., 2017. Ultrastructural characterization of membrane rearrangements induced by porcine epidemic diarrhea virus infection. Viruses 9, 251.
Zidar, N., Boštjančič, E., Jerala, M., Kojc, N., Drobne, D., Štabuc, B., Glavač, D., 2016. Down-regulation of microRNAs of the miR-200 family and up-regulation of Snail and Slug in inflammatory bowel diseases — hallmark of epithelial–mesenchymal transition. J. Cell Mol. Med. 20, 1813–1820.
Zong, Q.F., Huang, Y.J., Wu, L.S., Wu, Z.C., Wu, S.L., Bao, W.B., 2019. Effects of porcine epidemic diarrhea virus infection on tight junction protein gene expression and morphology of the intestinal mucosa in pigs. Pol. J. Vet. Sci. 22, 345–353.